

広島大学学術情報リポジトリ  
Hiroshima University Institutional Repository

Title	Robust Structurally Colored Coatings Composed of Colloidal Arrays Prepared by the Cathodic Electrophoretic Deposition Method with Metal Cation Additives
Author(s)	Katagiri, Kiyofumi; Uemura, Kensuke; Uesugi, Ryo; Tarutani, Naoki; Inumaru, Kei; Uchikoshi, Tetsuo; Seki, Takahiro; Takeoka, Yukikazu
Citation	ACS Applied Materials and Interfaces , 12 (36) : 40768 - 40777
Issue Date	2020-08-25
DOI	<a href="https://doi.org/10.1021/acsami.0c10588">10.1021/acsami.0c10588</a>
Self DOI	
URL	<a href="https://ir.lib.hiroshima-u.ac.jp/00049754">https://ir.lib.hiroshima-u.ac.jp/00049754</a>
Right	<p>This document is the Accepted Manuscript version of a Published Work that appeared in final form in ACS Applied Materials and Interfaces, copyright © American Chemical Society after peer review and technical editing by the publisher. To access the final edited and published work see <a href="https://doi.org/10.1021/acsami.0c10588">https://doi.org/10.1021/acsami.0c10588</a>.</p> <p>This is not the published version. Please cite only the published version. この論文は出版社版ではありません。引用の際には出版社版をご確認、ご利用ください。</p>
Relation	



# Robust Structurally Colored Coatings Composed of Colloidal Arrays Prepared by the Cathodic Electrophoretic Deposition Method with Metal Cation Additives

*Kiyofumi Katagiri,<sup>†,\*</sup> Kensuke Uemura,<sup>†</sup> Ryo Uesugi,<sup>†</sup> Naoki Tarutani,<sup>†</sup> Kei Inumaru,<sup>†</sup> Tetsuo Uchikoshi,<sup>‡</sup> Takahiro Seki,<sup>¶</sup> and Yukikazu Takeoka<sup>¶</sup>*

<sup>†</sup>Graduate School of Advanced Science and Engineering, Hiroshima University, 1-4-1 Kagamiyama, Higashi-Hiroshima 739-8527, Japan.

<sup>‡</sup> Research Center for Functional Materials, National Institute for Materials Science, 1-2-1 Sengen, Tsukuba 305-0047, Japan.

<sup>¶</sup> Graduate School of Engineering, Nagoya University, Furo-cho, Chikusa-ku, Nagoya 464-8603, Japan.

**ABSTRACT:** Structurally colored coatings composed of colloidal arrays of monodisperse spherical particles have attracted great attention owing to their versatile advantages, such as low-cost, resistance to fading, and low impacts on the environment and human health. However, the weak mechanical stability is considered to be a major obstacle for their practical applications as colorants. Although several approaches based on the addition of polymer additives to enhance the adhesion of particles have been reported, the challenge remains to develop a strategy for the preparation of structurally colored coatings with extremely high robustness using a simple process. Here, we have developed a novel approach to fabricate robust structurally colored coatings by using cathodic electrophoretic deposition (EPD). The addition of a metal salt, i.e.,  $\text{Mg}(\text{NO}_3)_2$ , to the coating dispersion allows  $\text{SiO}_2$  particles to have a positive charge, which enables the electrophoresis of  $\text{SiO}_2$  particles toward the cathode. At the cathode,  $\text{Mg}(\text{OH})_2$  co-deposits with  $\text{SiO}_2$  particles because  $\text{OH}^-$  ions are generated by the decomposition of dissolved oxygen and  $\text{NO}_3^-$  ions. The mechanical stability of the colloidal arrays obtained by this process is remarkably improved because  $\text{Mg}(\text{OH})_2$  facilitates the adhesion of the particles and substrates. The brilliant structural color is maintained even after several cycles of the sandpaper abrasion test. We have also demonstrated the coating on a stainless-steel fork. This demonstration reveals that our approach enables a homogeneous coating on a complicated surface. Furthermore, the high durability of the coating is clarified because the coating did not peel off even when the fork was stuck into a plastic eraser. Therefore, the coating technique developed here will provide an effective method for the pervasive application of structural color as a colorant.

## ■ INTRODUCTION

Inorganic pigments are commonly employed for various applications, such as paints, plastics, ceramics, and glasses, owing to their high thermal stability, hiding power, and weather resistance.<sup>1-3</sup> Most inorganic pigments, which have been previously used as colorants on an industrial scale, contain toxic metals, e.g., Cr, Hg, Cd, and Pb. These heavy metals are harmful not only to human health but also to the environment.<sup>3-8</sup> As a result of their high toxicity, the use of these toxic elements has become the subject of strict control through the imposition of legal regulations such as the Restriction of Hazardous Substances (RoHS).<sup>9</sup> In addition, governments of major developed countries have been legally executing agreements aimed at removing lead-containing pigments by 2020. Therefore, much effort has been devoted to eliminate the use of toxic heavy metals and also to produce a novel class of colorants.<sup>1,10,11</sup> In such efforts, structural colors have attracted great interest and extensive studies have been carried out in many fields.<sup>12-17</sup> Unlike the colors of pigments or dyes, structural colors originate from the interaction of visible light with nano- or microstructures, such as from scattering, reflection, diffuse reflection, diffraction, and interference. Therefore, they can be prepared using safe materials without the need to contain heavy metals and maintain their colors semi-permanently unless the structures of the materials are destroyed. These unique properties of structurally colored materials can provide numerous possibilities for their application in paints,<sup>18-20</sup> display devices,<sup>21-23</sup> colorimetric sensors,<sup>24,25</sup> smart windows,<sup>26</sup> optical filters,<sup>27</sup> and anti-counterfeiting.<sup>28,29</sup> Usually, nano- and microstructures with a modulation of the refractive index on the half scale of the wavelength of light are needed to obtain structural colors. One of the most versatile approaches, with high reproducibility, to fabricate such microstructures is an assembly of monodisperse spherical particles.<sup>13,17-19</sup> The colloidal arrays can provide structures

with high controllability over the whole range of visible light by simply changing the size of the particles. The preparation strategy of monodisperse spherical particles has already been well established. For example, monodisperse SiO<sub>2</sub> particles with desired sizes can easily be produced by the techniques based on the Stöber method.<sup>30</sup> Colloidal arrays can be categorized into two types.<sup>31</sup> The first is a colloidal crystal, which has long-range order in the array of the particles. The colloidal crystal exhibits glittering colors with strong iridescence, as seen in opals, so they are suitable for ornamental jewelry and the decoration of accessories. The other type of colloidal array is a colloidal amorphous array, which only has short-range order in the particle assembly. In contrast to a colloidal crystal, a colloidal amorphous array exhibits a relatively matt color with low iridescence, and is more comparable to pigmentary colors. Several methods, such as evaporation-based assembly,<sup>32</sup> thermal-assisted assembly,<sup>33</sup> drop-casting,<sup>34</sup> spin-coating,<sup>29</sup> centrifugation,<sup>35</sup> and spray coating techniques,<sup>36,37</sup> have been developed for the preparation of structurally colored materials composed of colloidal arrays. However, it is difficult to coat surfaces with a large area and/or complicated shapes using these methods. The electrophoretic deposition (EPD) method is a useful technique with great potential for a rapid, low-energy consumption, and cost-efficient coating technology for a wide range of surfaces.<sup>38-40</sup> The charged particles dispersed in the polar solvent migrate to the oppositely charged coating substrate by the application of a direct current (DC) voltage and then a colloidal array forms as a micrometer-thick layer. Therefore, EPD approaches have large potentials for colored coatings.<sup>41,42</sup> Recently, we have successfully achieved structurally colored coatings by using the EPD method.<sup>43,44</sup> Our approach has enabled the control of the thickness of the coating films over a large area, in contrast to that able to be achieved with other coating methods. In addition, we have demonstrated that both a colloidal crystalline array with iridescent structural colors and a

colloidal amorphous array with non-iridescent structural colors can be controllably prepared by varying the EPD conditions.<sup>44</sup> Nevertheless, the practical applications of structurally colored coatings are still hindered by the feeble mechanical durability of the colloidal arrays arising from the weak interaction among the particles. To enhance the mechanical persistence of the colloidal arrays, several approaches have been examined. Various kinds of polymers, such as poly(vinyl alcohol),<sup>45</sup> polyurea,<sup>46</sup> polyacrylate,<sup>47,48</sup> and chitosan,<sup>49</sup> have been added as binders to improve the mechanical stability of the colloidal arrays. We have proposed a technique which involves the addition of a cationic polyelectrolyte, poly(diallyldimethylammonium chloride) (PDDA), to the EPD system.<sup>44</sup> This technique enables us to prepare colloidal arrays through cationic EPD of SiO<sub>2</sub> particles, whereas anodic EPD is usually selected for the assembly of SiO<sub>2</sub> particles. PDDA acts as a binder and enhances the adhesion between the SiO<sub>2</sub> particles and the substrate. As a result, the coating film prepared by this cathodic EPD exhibits high abrasion resistance compared with that prepared by normal anionic EPD. Dhinojwala and co-workers have also reported structural colored coatings through the EPD of SiO<sub>2</sub> particles and co-deposition of polydopamine.<sup>50</sup> The co-deposited polydopamine can enhance the mechanical property. Nonetheless, the mechanical durability of the colloidal arrays with polymer binders is still not sufficient for practical applications. In addition, the intrinsic drawbacks of organic polymers, e.g., poor heat resistance, also limit their practical applications. Therefore, the development of a novel strategy for the preparation of colloidal arrays that have high mechanical robustness is of significant importance and necessity.

In this paper, a novel cathodic EPD process using metal cations is proposed to fabricate structurally colored coating films with extremely high abrasion resistance. The addition of cationic metal ions can invert the surface charge of SiO<sub>2</sub> particles in the coating dispersion from

negative to positive. Moreover, metal hydroxides are generated at the cathode along with the EPD of SiO<sub>2</sub> particles through the reaction of metal ions and hydroxyl ions generated on the cathodic surface. These metal hydroxides are expected to act as binders to adhere SiO<sub>2</sub> particles to each other and to the substrate. First, appropriate metal ions, which have a potential for the formation of homogenous colloidal arrays of SiO<sub>2</sub> particles through cathodic EPD, are examined. Next, the influence of the counter anions of metal salts on the formation of colloidal arrays is investigated. We also optimize the amount of metal salts added into the coating sols and the EPD conditions, such as applied voltage and duration. Finally, we compare the abrasion resistance of structurally colored coatings prepared by several EPD techniques, i.e., normal anodic EPD without any additives, cathodic EPD using polycation additives, and cathodic EPD using metal salts which is developed in this study.

## ■ EXPERIMENTAL SECTION

**Materials.** SiO<sub>2</sub> particles (average particle diameters: 200, 260, and 300 nm) were obtained from Fuji Chemical Co., Ltd (Osaka, Japan.). Each size of particles had a narrow size distribution. Fe<sub>3</sub>O<sub>4</sub> nanoparticles were provided by Toda Kogyo Corp. (Hiroshima, Japan.). Magnesium nitrate hexahydrate (Mg(NO<sub>3</sub>)<sub>2</sub>·6H<sub>2</sub>O; ≥99.0%), calcium nitrate tetrahydrate (Ca(NO<sub>3</sub>)<sub>2</sub>·4H<sub>2</sub>O; ≥98.5%), sodium nitrate (NaNO<sub>3</sub>; ≥99.0%), and magnesium sulfate heptahydrate (MgSO<sub>4</sub>·7H<sub>2</sub>O; ≥99.5%) were purchased from Kishida Chemical Co., Ltd. (Osaka, Japan.). Ammonium hydroxide solution (NH<sub>3</sub> aq.; 28 wt%) and 2-propanol (≥99.7%) were obtained from Nacalai Tesque, Inc. (Kyoto, Japan.). Hydrogen peroxide solution (H<sub>2</sub>O<sub>2</sub> aq.; 30 wt%) was purchased from Junsei Chemical Co., Ltd. (Tokyo, Japan.). All reagents were used as

received without further purification. Deionized water purified by a Millipore Milli-Q system (Merck Millipore, Billerica, MA, USA) was used in all experiments in this study.

**Preparation of coating sols for EPD.** Coating sols for EPD, i.e., dispersions containing SiO<sub>2</sub> particles and Fe<sub>3</sub>O<sub>4</sub> nanoparticles, were prepared as follows. First, SiO<sub>2</sub> particles (0.7g) were dispersed in 5 mL of the standard RCA-1 cleaning solution (5:1:1 H<sub>2</sub>O/H<sub>2</sub>O<sub>2</sub> aq./NH<sub>4</sub>OH aq. (v/v/v) mixture) with ultrasonication. Then the dispersion was heated at 60 °C for 30 min. This process was effective for the removal of organic substances from the surface of the SiO<sub>2</sub> particles owing to the solvating effect of NH<sub>4</sub>OH and the oxidizing effect of H<sub>2</sub>O<sub>2</sub>. As a result, the SiO<sub>2</sub> particles obtain sufficient hydrophilicity by activation of the Si-OH groups on the surface of the particles. The particles were centrifuged at 9390 × g for 5 min. After removal of the supernatant, the particles were redispersed in deionized water. This washing process was repeated twice. Next, the centrifuged SiO<sub>2</sub> particles were dispersed in 80 mL of 2-propanol with the assistance of ultrasonication. Then certain amounts of an aqueous dispersion of Fe<sub>3</sub>O<sub>4</sub> nanoparticles (2.5 wt%) were added to the dispersion. Finally, the EPD coating sols were completed by the addition of certain amounts of an aqueous solution of metal salts, e.g., Mg(NO<sub>3</sub>)<sub>2</sub>·6H<sub>2</sub>O, to the dispersion.

**Cathodic electrophoretic deposition.** A schematic representation of the EPD setup is shown in Fig. S1. Indium-tin oxide (ITO)-coated glass substrates were employed for EPD coating. Stainless-steel forks were used for the demonstration of the EPD coatings on a curved surface and complicated structure. The ITO-coated glass substrates were cleaned by the standard RCA-1 cleaning protocol, which was followed by rinsing with deionized water. Stainless-steel

wires (SUS304), which were shaped into spirals, were used as the counter electrodes. The coating substrate and the counter electrode were immersed in the coating sols. A specific voltage (10–40 V) was applied for a specific duration using a DC power supply (PAN110-3A, Kikusui Electronics Corp., Yokohama, Japan). An electrophoretic force toward the coating substrate was generated for the SiO<sub>2</sub> particles and Fe<sub>3</sub>O<sub>4</sub> nanoparticles by the application of a constant electric field. After electrophoresis, the substrates were withdrawn from the sols and dried at an ambient temperature.

**Characterization.** Optical images were taken using a digital camera to confirm the colors of the coatings. Scanning electron microscopy (SEM; Hitachi, S-4800) was employed to characterize the arrangement of the SiO<sub>2</sub> particles and the thickness of the EPD coating films. Pt sputter coatings were carried out before SEM observations. To observe the cross-sectional images, we cut the coating substrates using a diamond tip. The cutting position was fixed to 5 mm from the bottom of the substrate. The reflectance spectra of the coating films were measured using a UV-vis spectrometer (JASCO V-670) with an absolute reflectance measurement unit (ARMN-735). The surface robustness is a key feature that affects the practical application of structurally colored coatings. In this work, the sandpaper abrasion test was performed to evaluate the mechanical robustness of the coating films. A diagrammatic illustration of the sandpaper abrasion test is shown in Fig. 1. The coated substrates were placed face-down on sandpaper (600 mesh) and a 100-g weight was placed on top of the substrate. The sample was moved 3 cm in a straight manner at a rate of 1 cm sec<sup>-1</sup>, and this was defined as one cycle. The residual areas of the structurally colored coating films were evaluated after every abrasion test cycle.

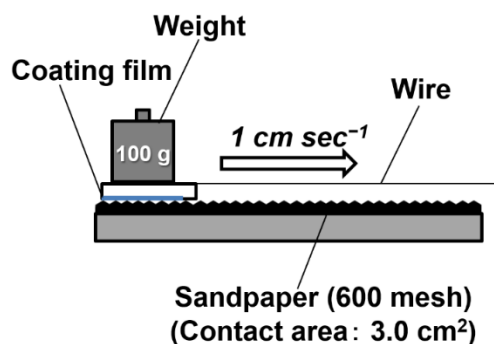


**Figure 1.** Schematic representation of the sandpaper abrasion test for the coating film on an ITO-coated glass substrate.

## ■ RESULTS AND DISCUSSION

**Selection of metal salts.** In this study, the metal cations were expected to have two roles. The primary role was as an agent to allow SiO<sub>2</sub> particles and Fe<sub>3</sub>O<sub>4</sub> nanoparticles to possess positive charges.<sup>51–53</sup> The other role was to enhance the adhesion of the deposited films onto the substrate by forming metal hydroxides as binders.<sup>54</sup> First, we examined three nitrate salts, NaNO<sub>3</sub>, Ca(NO<sub>3</sub>)<sub>2</sub>, and Mg(NO<sub>3</sub>)<sub>2</sub>, as additives for the coating sols of EPD. Optical photographic images of the coating films prepared from the sols containing various salts, i.e., NaNO<sub>3</sub>, Ca(NO<sub>3</sub>)<sub>2</sub>, or Mg(NO<sub>3</sub>)<sub>2</sub>, are shown in Fig. 2. The amount of the salts was fixed at  $7.5 \times 10^{-4}$  mol g<sup>-1</sup> (vs. weight of SiO<sub>2</sub> particles in the coating sols). SiO<sub>2</sub> particles with a diameter of 200 nm were employed. The zeta-potential of the employed SiO<sub>2</sub> particles in the neutral aqueous medium without any additives was -64.5 mV. The applied voltage and EPD duration were fixed at 20 V and 5 min, respectively. When NaNO<sub>3</sub> was added to the coating sol, no film formation was confirmed (Fig. 2a). However, homogeneous coating films that exhibited vivid blue structural color were obtained by cathodic EPD from coating sols containing Ca(NO<sub>3</sub>)<sub>2</sub> and Mg(NO<sub>3</sub>)<sub>2</sub> (Fig.

2b, c). The zeta-potentials of SiO<sub>2</sub> particles under these conditions were -40.6 mV (NaNO<sub>3</sub>), +21.2 mV (Ca(NO<sub>3</sub>)<sub>2</sub>), and +48.2 mV(Mg(NO<sub>3</sub>)<sub>2</sub>). The surface charge of the SiO<sub>2</sub> particles was inverted to be positive when divalent cations, i.e., Ca<sup>2+</sup> or Mg<sup>2+</sup>, were added. Therefore, it was expected that the adsorption of Ca<sup>2+</sup> or Mg<sup>2+</sup> afforded a positive charge to the SiO<sub>2</sub> particles. However, Na<sup>+</sup> did not have the ability to invert the surface charge of SiO<sub>2</sub> particles from negative to positive because it is a monovalent cation.

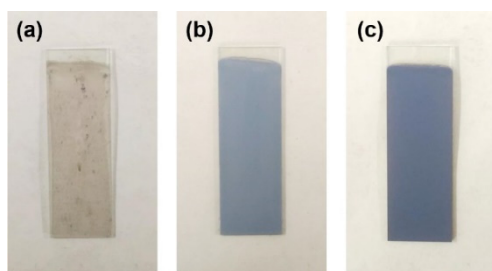


**Figure 2.** Optical photographic images of coating films prepared by cathodic EPD using various metal nitrate salts as additives. The metal salt additives are (a) NaNO<sub>3</sub>, (b) Ca(NO<sub>3</sub>)<sub>2</sub>, and (c) Mg(NO<sub>3</sub>)<sub>2</sub>. The size of SiO<sub>2</sub> particles used here is 200 nm. The quantity of metal salts in the coating sols is  $7.5 \times 10^{-4}$  mol g<sup>-1</sup> (vs. weight of SiO<sub>2</sub> particles). The EPD voltage and duration are 20 V and 5 min, respectively.

The surface morphology of the coating films prepared by cathodic EPD from coating sols containing Ca(NO<sub>3</sub>)<sub>2</sub> and Mg(NO<sub>3</sub>)<sub>2</sub> was observed by SEM (Fig. S2). Particle arrays with disordered arrangements (without long-range orders) were observed for both films. When cathodic EPD was carried out in the presence of Ca<sup>2+</sup>, small deposits, which differed from SiO<sub>2</sub> particles, were observed (Fig. S2a). These deposits were predicted to be Ca(OH)<sub>2</sub>, which was

generated through the reaction of  $\text{Ca}^{2+}$  and  $\text{OH}^-$  during the EPD process.  $\text{Ca}(\text{OH})_2$  was deposited inhomogeneously on the  $\text{SiO}_2$  particle arrays and the particles were not interconnected. However, the deposits, which were predicted to be  $\text{Mg}(\text{OH})_2$ , were generated homogeneously into the voids of the  $\text{SiO}_2$  particles and the particles were partially interconnected when the coating films were prepared by cathodic EPD in the presence of  $\text{Mg}^{2+}$  (Fig. S2b). This difference of the generation of metal hydroxides on the voids in the particle array probably arose from the difference in the solubility between  $\text{Mg}(\text{OH})_2$  and  $\text{Ca}(\text{OH})_2$  in water. The solubility of  $\text{Mg}(\text{OH})_2$  in water (0.00122 g/100 mL (at 25 °C)) is much lower than that of  $\text{Ca}(\text{OH})_2$  in water (0.16 g/100 mL (at 25 °C)).<sup>55</sup> Therefore, the formation of  $\text{Mg}(\text{OH})_2$  was caused quickly and homogeneously when the  $\text{SiO}_2$  particles surrounded with  $\text{Mg}^{2+}$  reached the electrode surface by electrophoresis. The sandpaper abrasion test was carried out to compare the mechanical abrasion resistance of the coating films. Fig. 3 shows optical photographs of the cathodic EPD coating films prepared using  $\text{Ca}^{2+}$  and  $\text{Mg}^{2+}$  before and after the sandpaper abrasion test (1, 2, and 3 cycles). The remaining area of the coating films after the abrasion test as a function of test cycles is also shown in Fig. 3. The coating film prepared using  $\text{Ca}^{2+}$  began to peel (nearly 80%) after only one cycle of sandpaper abrasion. After three cycles, the coating was completely abraded (Fig. 3a, c). This result revealed that the adhesion between the coating and the substrate was relatively low. However, more than 90% of the coating films (in area) remained even after three cycles of sandpaper abrasion for the sample prepared using  $\text{Mg}^{2+}$  (Fig. 3b, c). Therefore,  $\text{Mg}^{2+}$  is a preferable cation as an additive for cathodic EPD to prepare coating films composed of arrays of  $\text{SiO}_2$  particles with high mechanical abrasion resistance.

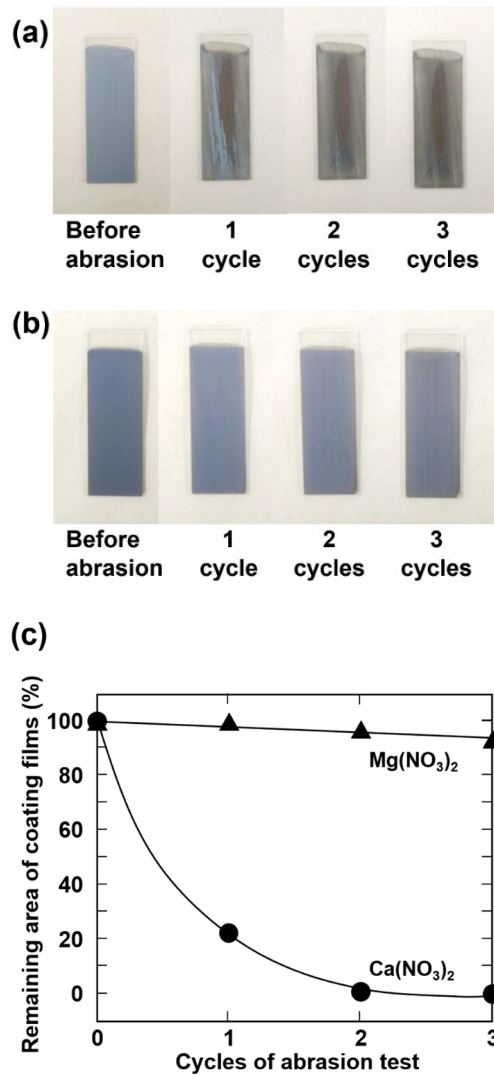


**Figure 3.** Optical photographic images of the EPD coating films prepared by cathodic EPD using (a)  $\text{Ca}(\text{NO}_3)_2$  and (b)  $\text{Mg}(\text{NO}_3)_2$  before and after the sandpaper abrasion test (1, 2, and 3 cycles). (c) Remaining area of coating films after abrasion test as a function of test cycles for coating films prepared by cathodic EPD using  $\text{Ca}(\text{NO}_3)_2$  and  $\text{Mg}(\text{NO}_3)_2$ .  $\text{SiO}_2$  particles with a diameter of 200 nm were used. The quantity of metal salts in the coating sols is  $7.5 \times 10^{-4} \text{ mol g}^{-1}$  (vs. weight of  $\text{SiO}_2$  particles). The EPD voltage and duration are 20 V and 5 min, respectively.

Next, the influence of the counter anions of the Mg salts employed for the cathodic EPD coatings was investigated. Fig. 4 shows optical photographic images of the films prepared using  $\text{MgSO}_4$ ,  $(\text{CH}_3\text{COO})_2\text{Mg}$ , and  $\text{Mg}(\text{NO}_3)_2$ . The amount of the salts was fixed to  $7.5 \times 10^{-4} \text{ mol g}^{-1}$  (vs. weight of  $\text{SiO}_2$  particles in the coating sols). The applied voltage and EPD duration were fixed to 20 V and 5 min, respectively. When  $\text{MgSO}_4$  was employed as a salt containing  $\text{Mg}^{2+}$ , a coating film composed of arrays of  $\text{SiO}_2$  particles was not obtained (Fig. 4a). In contrast, a coating film was formed by cathodic EPD using  $(\text{CH}_3\text{COO})_2\text{Mg}$ . The film and its structural color were not homogeneous as shown in Fig. 4b. However, a homogeneous coating film that exhibited a vivid blue structural color was generated by cathodic EPD from the coating sol containing  $\text{Mg}(\text{NO}_3)_2$  (Fig. 4c).

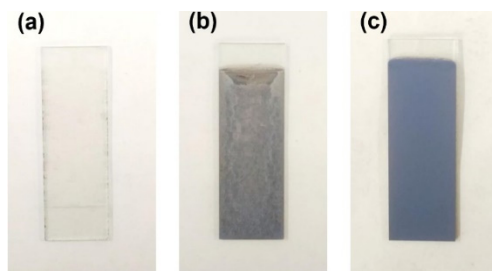
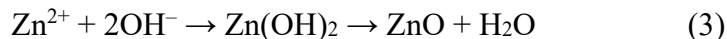
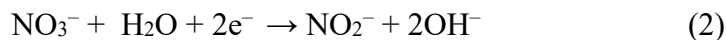


**Figure 4.** Optical photographic images of the EPD coating films prepared by cathodic EPD using Mg salts as additives. The Mg salt additives are (a)  $\text{MgSO}_4$ , (b)  $(\text{CH}_3\text{COO})_2\text{Mg}$ , and (c)  $\text{Mg}(\text{NO}_3)_2$ . The size of  $\text{SiO}_2$  particles used here is 200 nm. The quantity of metal salts in the coating sols is  $7.5 \times 10^{-4} \text{ mol g}^{-1}$  (vs. weight of  $\text{SiO}_2$  particles). The EPD voltage and duration are 20 V and 5 min, respectively.

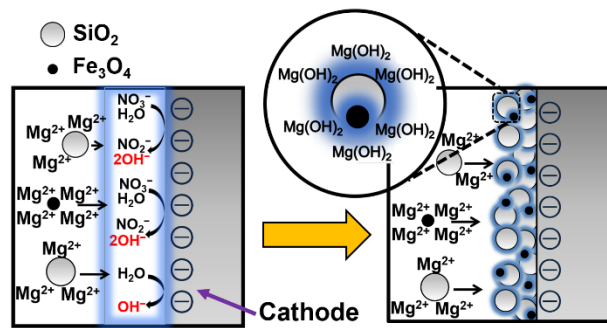
Judging from these results, nitrate is a preferable anion of the Mg salt for the formation of homogeneous particle arrays on the cathode by the EPD process. Actually, nitrate salts have been most commonly employed for the preparation of metal oxide films by the electrochemical deposition technique. For example, Izaki and co-workers reported the preparation of transparent ZnO films by an electrochemical reaction using  $\text{Zn}(\text{NO}_3)_2$ .<sup>56,57</sup> The deposition reactions of the ZnO film on a cathode substrate are described by the following equations:



Eqs (1) and (2) suggest that the local pH increase in the vicinity of the cathode during the electric field application for the solution containing metal nitrate is caused by reduction reactions not only of dissolved oxygen but also of a nitrate ion. A schematic illustration of the chemical reaction during the application of an electric field is shown in Fig. 5. On the surface of the cathode, the local pH increased by the reactions of Eqs (1) and (2). The formation of  $\text{Mg}(\text{OH})_2$  occurred accompanied with the deposition of  $\text{SiO}_2$  and  $\text{Fe}_3\text{O}_4$  particles according to Eq. (4) in the vicinity of the cathode.

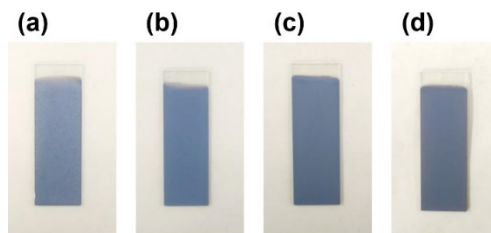


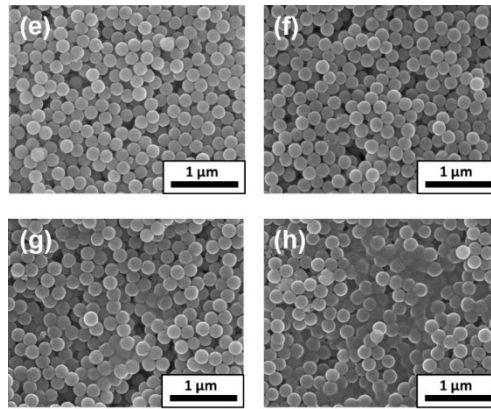
Therefore, the use of  $\text{Mg}(\text{NO}_3)_2$  seems to be suitable for the formation of  $\text{Mg}(\text{OH})_2$  in the voids of an electrophoretically-deposited  $\text{SiO}_2$  particles array on the cathode in our system, and we employed  $\text{Mg}(\text{NO}_3)_2$  as an additive for the cathodic EPD experiments in this study. The colors of the coating films were able to be controlled simply by changing the size of  $\text{SiO}_2$  particles. By cathodic EPD using a  $\text{Mg}(\text{NO}_3)_2$  additive, homogeneous coating films with blue, green, and red colors could be fabricated from  $\text{SiO}_2$  particles with diameters of 200, 260, and 300 nm, respectively (Fig. S3). These colors were in accordance with the coating films prepared by anodic EPD or cathodic EPD using PDDA, as reported in our previous papers.<sup>43,44</sup> The angle-resolved optical properties of the coating films were examined to quantify the angle dependence of the structural color. Fig. S4 shows the reflection spectra of the coating films corresponding to the change in the measurement angle. The shifts of the positions of peak wavelengths in these reflection spectra were low even when the detection angle was varied from 10 to 60°. These results suggest that the films were composed of colloidal amorphous arrays. Hereafter,  $\text{SiO}_2$  particles with diameters of 200 nm were employed representatively for the further examinations.



**Figure 5.** Schematic representation of chemical decomposition of  $\text{H}_2\text{O}$  and  $\text{NO}_3^-$ , and deposition of  $\text{SiO}_2$  and  $\text{Fe}_3\text{O}_4$  particles with  $\text{Mg}(\text{OH})_2$  on the surface of the cathode during application of an electric field.

**Influence of the quantity of  $\text{Mg}(\text{NO}_3)_2$ .** Next, the influences of the concentration of  $\text{Mg}(\text{NO}_3)_2$  on the formation of the coating films were investigated. Fig. 6 shows the optical photographic images and surface SEM images of the coating films prepared by cathodic EPD from sols with various quantities of  $\text{Mg}(\text{NO}_3)_2$ , i.e.,  $0.5\text{--}7.5 \times 10^{-4} \text{ mol g}^{-1}$  (vs. weight of  $\text{SiO}_2$  particles in the coating sols). The applied voltage and duration of the deposition were fixed at 20 V and 5 min, respectively. Homogeneous coating films with a vivid blue color were obtained by cathodic EPD even in the case of a lower  $\text{Mg}(\text{NO}_3)_2$  concentration ( $0.5 \times 10^{-4} \text{ mol g}^{-1}$ ). The color was derived from the coherent light scattering from the array of particles with a size of 200 nm. The observed color appeared to be almost the same regardless of the concentration of  $\text{Mg}(\text{NO}_3)_2$  in the coating sols. However, differences were found for the morphology of the obtained films with the concentration of  $\text{Mg}(\text{NO}_3)_2$ . From the SEM images of the coating films prepared with a lower  $\text{Mg}(\text{NO}_3)_2$  concentration ( $\leq 0.5 \times 10^{-4} \text{ mol g}^{-1}$ ), only arrays of  $\text{SiO}_2$  particles with the short-range order were observed (Fig. 6e). In contrast, it was observed that the voids between  $\text{SiO}_2$  particles were partially filled with another substance, i.e.,  $\text{Mg}(\text{OH})_2$ , in the case of the coating films prepared with a higher  $\text{Mg}(\text{NO}_3)_2$  concentration ( $\geq 5.0 \times 10^{-4} \text{ mol g}^{-1}$ ) (Fig. 6g, h).

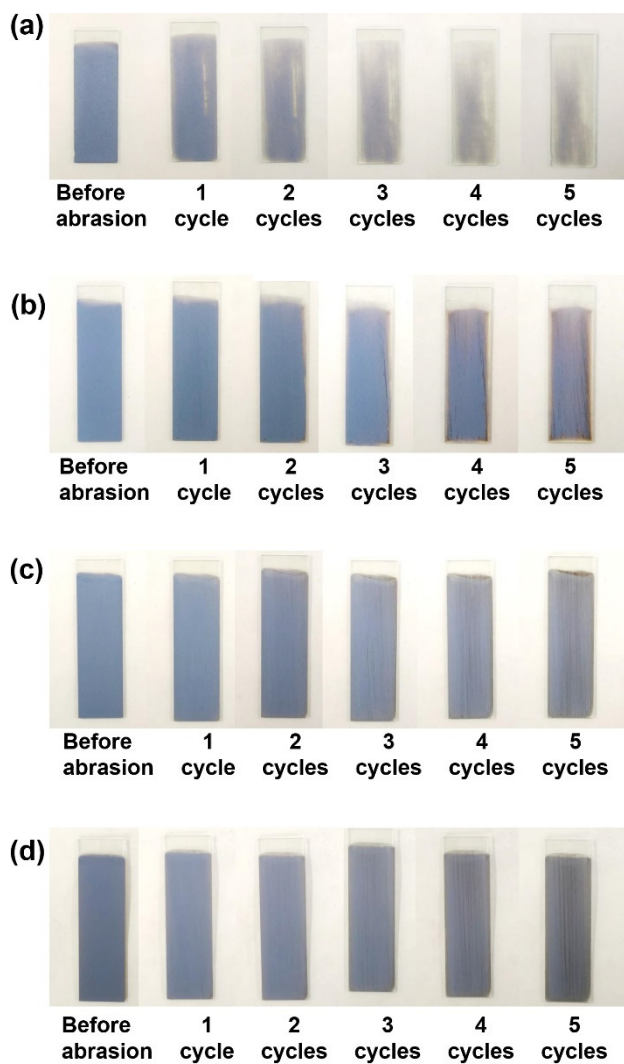


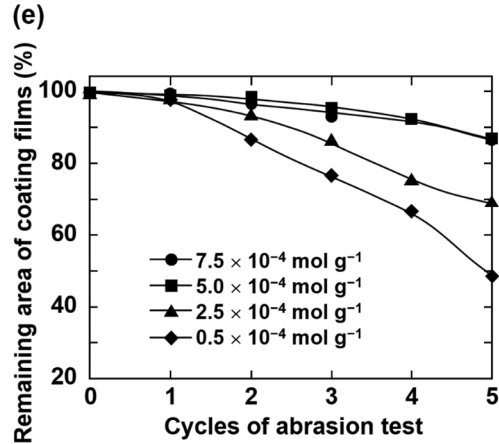


**Figure 6.** (a–d) Optical photographic images and (e–h) surface SEM images of the EPD coating films prepared by cathodic EPD using  $\text{Mg}(\text{NO}_3)_2$  as additive. The quantities of  $\text{Mg}(\text{NO}_3)_2$  are (a,e)  $0.5 \times 10^{-4}$ , (b,f)  $2.5 \times 10^{-4}$ , (c,g)  $5.0 \times 10^{-4}$ , and (d,h)  $7.5 \times 10^{-4} \text{ mol g}^{-1}$  (vs. weight of  $\text{SiO}_2$  particles in the coating sols). The size of  $\text{SiO}_2$  particles used here is 200 nm. The EPD voltage and duration are 20 V and 5 min, respectively.

The deposited  $\text{Mg}(\text{OH})_2$  was able to connect  $\text{SiO}_2$  particles with each other and enhance the adhesion of particle arrays on the substrate. Therefore, the concentration of  $\text{Mg}(\text{NO}_3)_2$  of the coating sols should affect the mechanical abrasion resistance of the resultant EPD coating films. Fig. 7 shows optical photographs of the cathodic EPD coating films prepared with various  $\text{Mg}^{2+}$  concentrations before and after the sandpaper abrasion test (1, 2, 3, 4, and 5 cycles). The remaining area of the coating films as a function of abrasion test cycles is also shown in Fig. 7. After one abrasion cycle, the remaining areas of the coating films were more than 98% regardless of the concentration of  $\text{Mg}(\text{NO}_3)_2$  of the coating sols. In the case of the coating film prepared from coating sols with a lower  $\text{Mg}(\text{NO}_3)_2$  concentration ( $0.5 \times 10^{-4} \text{ mol g}^{-1}$ ), the remaining area of the coating films diminished stepwise with each abrasion test cycle and the

remaining area after five abrasion test cycles was less than 50% (Fig. 7a). Even for the case when the  $\text{Mg}(\text{NO}_3)_2$  concentration was  $2.5 \times 10^{-4} \text{ mol g}^{-1}$ , more than 30% (in area) of the coating film was abraded after five test cycles (Fig. 7b). However, more than 85% of the coating films (in area) prepared using coating sols with a higher  $\text{Mg}^{2+}$  concentration ( $\geq 5.0 \times 10^{-4} \text{ mol g}^{-1}$ ) remained even after five cycles of abrasion testing (Fig. 7c, d).

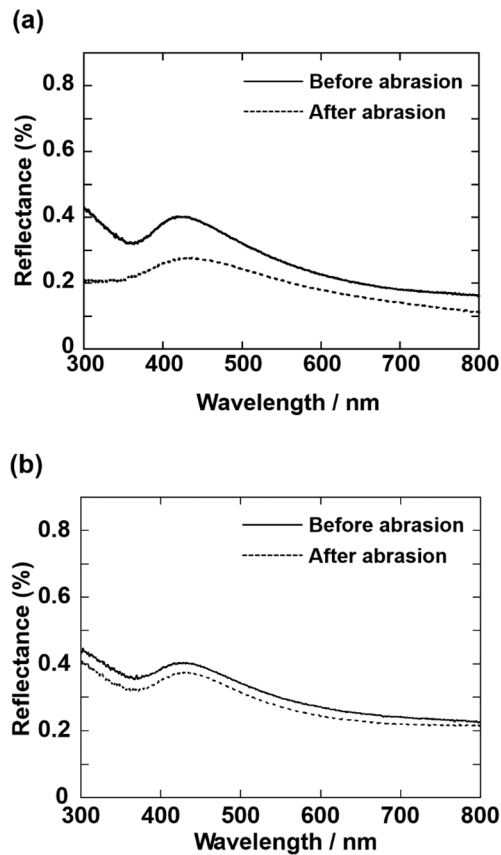




**Figure 7.** Optical photographic images of the EPD coating films prepared by cathodic EPD using  $\text{Mg}(\text{NO}_3)_2$  as additive before and after the sandpaper abrasion test (1, 2, 3, 4, and 5 cycles). The quantities of  $\text{Mg}(\text{NO}_3)_2$  are (a)  $0.5 \times 10^{-4}$ , (b)  $2.5 \times 10^{-4}$ , (c)  $5.0 \times 10^{-4}$ , and (d)  $7.5 \times 10^{-4} \text{ mol g}^{-1}$  (vs. weight of  $\text{SiO}_2$  particles in the coating sols). (e) Remaining area of coating films after abrasion test as a function of test cycles for the coating films. The size of  $\text{SiO}_2$  particles used here is 200 nm. The EPD voltage and duration are 20 V and 5 min, respectively.

The quantitative reflectance spectra of the coating films before and after five cycles of the abrasion test are shown in Fig. 8. The coating films were prepared with  $\text{Mg}(\text{NO}_3)_2$  concentrations of  $2.5 \times 10^{-4}$  and  $7.5 \times 10^{-4} \text{ mol g}^{-1}$ . Before the abrasion tests, the reflection peak ascribed to coherent light scattering from the array of  $\text{SiO}_2$  particles with a diameter of 200 nm was clearly observed in the spectra of both samples. For the coating film prepared with an  $\text{Mg}(\text{NO}_3)_2$  concentration of  $2.5 \times 10^{-4} \text{ mol g}^{-1}$ , the peak intensity decreased drastically after the five cycles of the abrasion test (Fig. 8a). In addition, the reflection was also suppressed over the entire

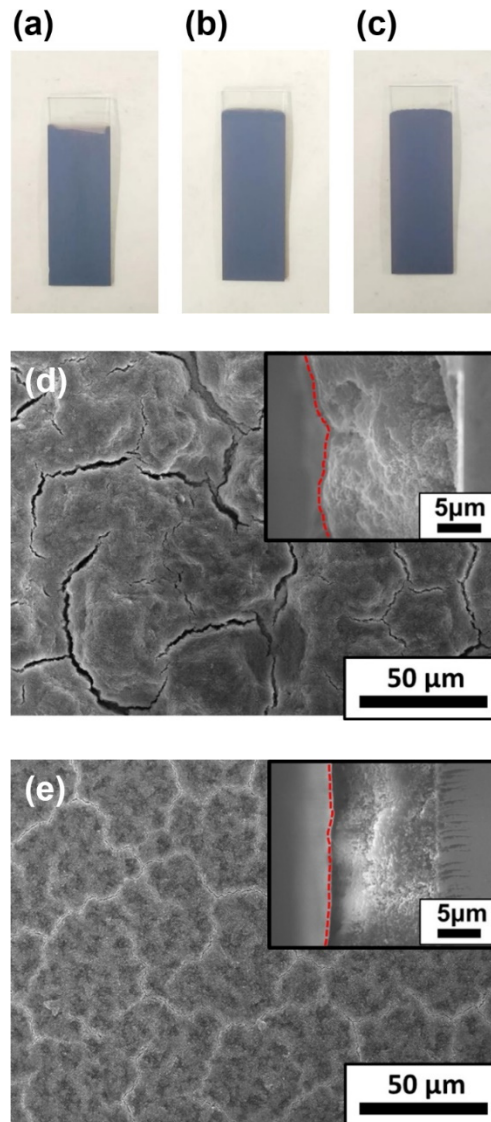
wavelength range. This indicated that the film thickness was reduced by the abrasion test and the robustness of the film prepared by this condition was not very high. In contrast, the changes in the spectral shape were negligible even after the five cycles of the abrasion test for the coating film prepared with an  $\text{Mg}(\text{NO}_3)_2$  concentration of  $7.5 \times 10^{-4} \text{ mol g}^{-1}$  (Fig. 8b). Therefore, the coating film exhibited a high robustness and maintained a sufficient thickness after the abrasion test. Based on these results, the concentration of  $\text{Mg}(\text{NO}_3)_2$  to add to the coating sols should be more than  $5.0 \times 10^{-4} \text{ mol g}^{-1}$ , and we fixed the concentration of  $\text{Mg}(\text{NO}_3)_2$  to  $7.5 \times 10^{-4} \text{ mol g}^{-1}$  for the following experiments.



**Figure 8.** Reflectance spectra of the coating films prepared by cathodic EPD using  $\text{Mg}(\text{NO}_3)_2$  as additive before and after the sandpaper abrasion test. The quantities of  $\text{Mg}(\text{NO}_3)_2$  are (a)  $2.5 \times 10^{-4}$  and (b)  $7.5 \times 10^{-4}$  mol  $\text{g}^{-1}$  (vs. weight of  $\text{SiO}_2$  particles in the coating sols). The size of  $\text{SiO}_2$  particles used here is 200 nm. The EPD voltage and duration are 20 V and 5 min, respectively.

**Influence of the EPD conditions.** We investigated the influence of the applied voltage for EPD on the morphology of the coating films. The voltage was varied from 10 to 40 V. The duration of EPD was fixed at 5 min. Optical photographs and surface SEM images of the coating films prepared with various applied voltages are shown in Fig. 9. In addition, cross-sectional SEM images of the coating films prepared with applied voltages of 10 and 20 V are given as insets. As seen in Fig. 9a–c, the coatings exhibited a vivid blue structural color regardless of the applied voltages for the EPD process and the appearance of these films had almost no difference. However, there were appreciable differences in the morphology of the coating films at the micrometer- scale. When the applied voltage was 10 V, cracks with a size of 50  $\mu\text{m}$  were observed in the surface SEM image (Fig. 9d). An uneven thickness was also observed in the cross-sectional SEM image. In the case of the coating film prepared with a higher applied voltage (40 V), there were a number of pinholes in the surface SEM image, though the size of the cracks decreased (Fig. 9f). The pinholes were proposed to be generated by the formation of  $\text{H}_2$  gas from water electrolysis on the cathode owing to the high applied voltage. In contrast, no large cracks and pinholes were detected from the surface SEM image of the coating film prepared at 20 V (Fig. 9e). In addition, the cross-sectional image revealed that the morphology of the film in the direction of the depth was homogeneous. Here, 2-propanol was employed as the

main dispersant. Only a small amount of water was added to the coating sol as a solvent of  $\text{Mg}(\text{NO}_3)_2$ . Therefore, water electrolysis was suppressed even when the applied voltage was relatively high, such as 20 V. Therefore, we decided that the optimal applied voltage for the current EPD system was 20 V.



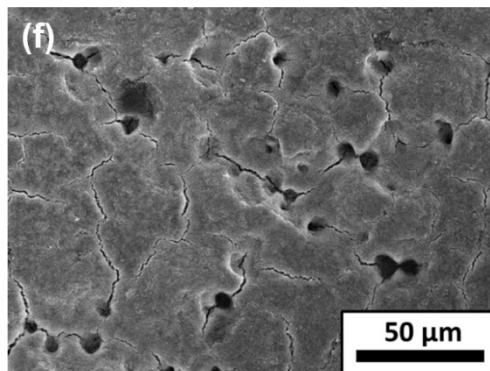


**Figure 9.** (a–c) Optical photographic images and (d–f) surface SEM images of the EPD coating films prepared by cathodic EPD using  $\text{Mg}(\text{NO}_3)_2$  ( $7.5 \times 10^{-4} \text{ mol g}^{-1}$ , vs. weight of  $\text{SiO}_2$  particles in the coating sols). The insets in (e) and (f) are cross-sectional SEM images of corresponded films. The size of  $\text{SiO}_2$  particles used here is 200 nm. The applied voltages are (a,d) 10, (b, e) 20, and (c, f) 40 V. The EPD duration is 5 min.

Next, we examined the influence of the duration of EPD on the thickness of the coating films. The duration was varied from 10 sec to 8 min. Optical photographs and the increases of the film thickness as a function of EPD duration are shown in Fig. 10. The cross-sectional SEM images of the coating films prepared with various EPD durations are also given in Fig. S5. The coating film obtained from a short EPD duration (10 and 30 sec) exhibited a faint structural color. The thickness of the film prepared by EPD for 30 sec was ca. 4  $\mu\text{m}$  (Fig. 10b and Fig. S5b). It was proposed that the coherent light scattering generated from the film with such a thickness was not sufficient. The film thickness increased proportional to the EPD duration until 1 min. The thickness reached 9  $\mu\text{m}$  when the EPD duration was 1 min. The film exhibited a brilliant structural color. When the total EPD duration was extended to 2 min, the additional increase of the thickness was only 1  $\mu\text{m}$ . Moreover, the film thickness did not grow even when the EPD

duration was extended to 5 or 8 min (Fig. 10b). When the EPD duration was prolonged, the deposition amount of  $\text{Mg}(\text{OH})_2$  in the voids of  $\text{SiO}_2$  particles increased, until the surface of the cathodic electrode was completely covered with insulating substance, i.e.,  $\text{Mg}(\text{OH})_2$ . As a result, the electric field between anode and cathode decayed and the electrophoresis of  $\text{SiO}_2$  particles was suppressed. Therefore, these results revealed that our cathodic EPD system enables a control of the thickness of the coating films by the EPD duration, but there is a limit for the maximum thickness.

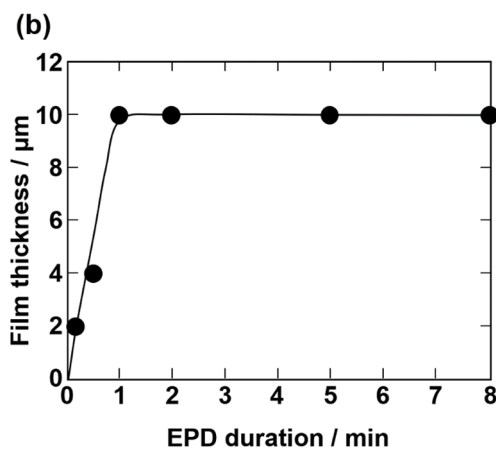
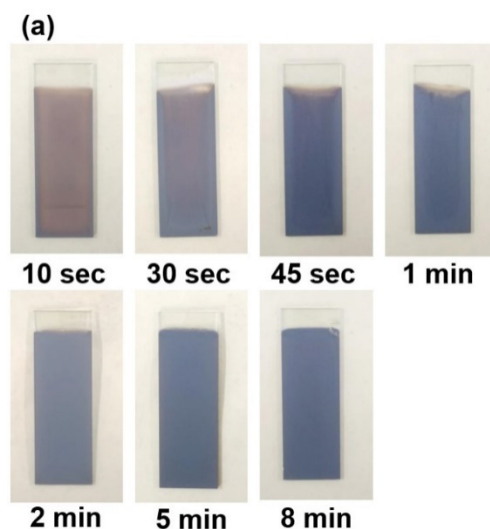


**Figure 10.** (a) Optical photographic images of the EPD coating films prepared by cathodic EPD using  $\text{Mg}(\text{NO}_3)_2$  ( $7.5 \times 10^{-4} \text{ mol g}^{-1}$ , vs. weight of  $\text{SiO}_2$  particles in the coating sols). (b) Thickness of the EPD coating films as a function of the EPD durations. The size of  $\text{SiO}_2$  particles used here is 200 nm. The EPD duration is 10 sec, 30 sec, 45 sec, 1 min, 2 min, 5 min, and 8 min. The applied voltage is 40 V.

### **Comparison of anti-abrasion property of coating films prepared by various EPD systems.**

The robustness of the structurally colored coatings is a very important feature for the widespread application. A total of five cycles of the sandpaper abrasion test were conducted to evaluate the mechanical stability of the colloidal arrays prepared by the various EPD methods. The coating film was prepared by cathodic EPD using  $\text{Mg}(\text{NO}_3)_2$  ( $7.5 \times 10^{-4} \text{ mol g}^{-1}$ ) at 20 V for 5 min. For comparison, the coating films prepared by anodic EPD without any additives<sup>43</sup> and by cathodic EPD using a polycation (PDDA)<sup>44</sup> were also analyzed. For the anodic EPD, the EPD applied voltage and duration were 90 V and 1 min, respectively. The quantity of PDDA in the coating sols was  $5.9 \times 10^{-3} \text{ wt}\%$  in the case of cathodic EPD using a polycation (PDDA). In this case, the EPD applied voltage and duration were 7 V and 8 min, respectively. Optical photographic images of the coating films prepared by anodic EPD, cathodic EPD using polycation (PDDA), and cathodic EPD using  $\text{Mg}(\text{NO}_3)_2$  before and after the sandpaper abrasion test (1, 2, 3, 4, and 5 cycles) are shown in Fig. 11. The remaining area of the coating films after the abrasion test as a function of test cycles are also shown in Fig. 11. The coating film prepared by the anodic EPD process was completely scratched-off after only one cycle of the sandpaper abrasion test, which showed a weak adhesion between the  $\text{SiO}_2$  particles with each other and with the substrate without adhesive. In the case of the coating film prepared by cathodic EPD using PDDA, ca.

90% of the coating film remained after one cycle of the abrasion test; nevertheless, the film was almost completely peeled off after five cycles of the abrasion test (Fig. 11b). However, the coating films prepared by the cathodic EPD process using  $Mg(NO_3)_2$  remained intact even after five cycles of abrasion testing (Fig. 11c).

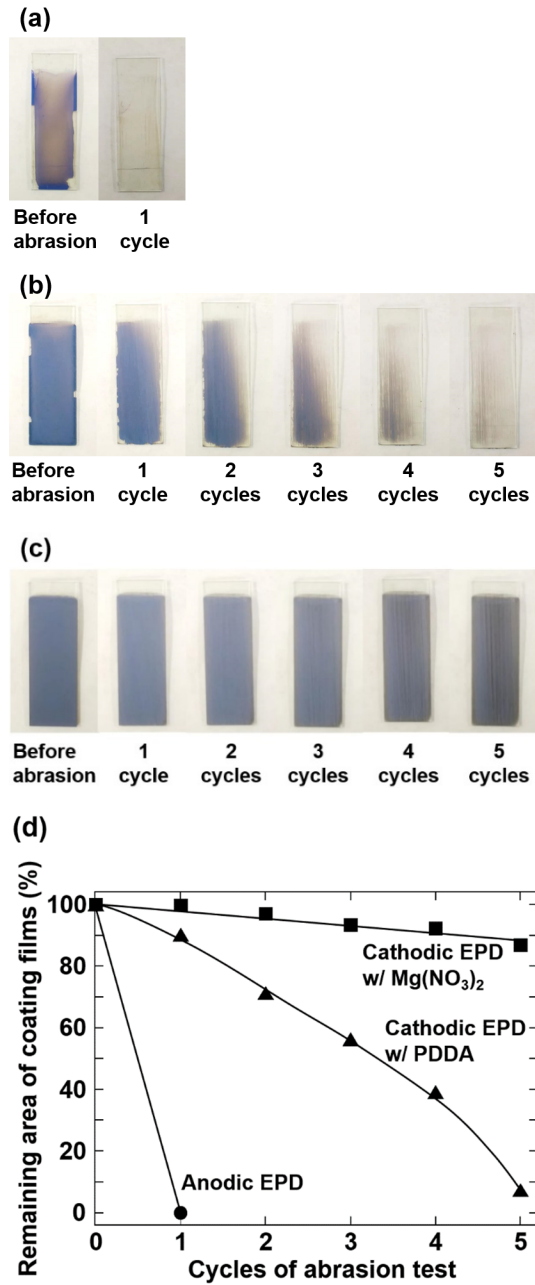


**Figure 11.** Optical photographic images of the coating films prepared by (a) anodic EPD, (b) cathodic EPD using PDDA, and (c) cathodic EPD using  $\text{Mg}(\text{NO}_3)_2$  as additives before and after the sandpaper abrasion test (1, 2, 3, 4, and 5 cycles). (d) Remaining area of coating films after the abrasion test as a function of test cycles for the coating films. The size of  $\text{SiO}_2$  particles used here is 200 nm.

Further examination of the robustness of the coating films was performed by using stainless-steel forks and a plastic eraser. The stainless-steel forks were employed as coating substrate materials for EPD. The coating films prepared by both anodic EPD and cathodic EPD using  $\text{Mg}(\text{NO}_3)_2$  displayed homogeneous coatings with a vivid blue structural color. The robustness was examined by sticking the coated forks into the eraser. As shown in Fig. 12a and Mov. S1, flakes of the coating films prepared by anodic EPD easily peeled-off from the fork when it was stuck into the eraser. After pulling out the fork from the eraser, the bare metal surface of the fork was observed. This indicated that the mechanical stability of the coating film was low. In contrast, the blue structurally colored coating on the fork remained intact after the stick and pull test using the eraser when the film was coated by cathodic EPD using  $\text{Mg}(\text{NO}_3)_2$  (Fig. 12b and Mov. S2). This result showed that this coating has sufficient mechanical stability against abrasion.

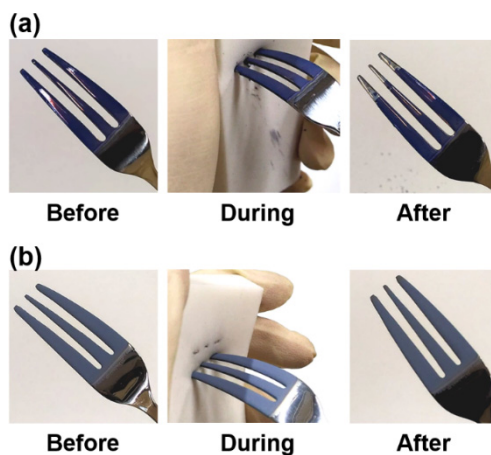


**Figure 12.** Optical photographic images of the EPD coating films on stainless-steel forks by (a) anodic EPD and (b) cathodic EPD using  $Mg(NO_3)_2$  as additive before, during, and after sticking into the eraser. The size of the  $SiO_2$  particles used here is 200 nm.

## ■ CONCLUSIONS

In summary, we have developed a facile method to fabricate robust coating films which can exhibit vivid structural colors. The films composed of arrays of monodisperse spherical  $SiO_2$  particles can be successfully constructed by the EPD process. The addition of  $Mg^{2+}$  ions allows the  $SiO_2$  particles to possess a positive charge in the dispersions and enables cathodic EPD for the formation of the particles array. The local pH increases in the vicinity of the cathode during the EPD process, which is caused by reduction reactions not only of dissolved oxygen but also of the nitrate ion added as a counter anion of the Mg salt. As a result,  $Mg(OH)_2$  co-deposits into the voids of the  $SiO_2$  particles array, which forms a strong adhesion between the particles and the substrate. The deposition amount of  $Mg(OH)_2$  within the particles array is affected by the concentration of  $Mg(NO_3)_2$  in the coating sols. The coating films exhibit a noniridescent

structural color that originates from the coherent light scattering from the particles array with a short-range order. The structural color can endure cycles of the sandpaper abrasion test. The mechanical strength of the coating films prepared by this EPD process surpasses that prepared by a previous EPD approach, which includes cathodic EPD using polymer additives. Moreover, because all the components of the films are inorganic materials, i.e.,  $\text{SiO}_2$ ,  $\text{Fe}_3\text{O}_4$ , and  $\text{Mg}(\text{OH})_2$ , an improvement of the robustness of the coating films can be expected not only for the mechanical stability but also for other features, including heat-resistance. Therefore, this system can provide novel perspectives as a sustainable coloring technique for various kinds of applications in paints and external decorations.

## ■ ASSOCIATED CONTENT

### Supporting Information

Schematic representation of the setup for the EPD system. Surface SEM images of coating films prepared by cathodic EPD using  $\text{Ca}(\text{NO}_3)_2$  and  $\text{Mg}(\text{NO}_3)_2$ . Optical photographic images and reflection spectra of the EPD coating films prepared using  $\text{SiO}_2$  particles with various diameters. Cross-sectional SEM images of the EPD coating films prepared by cathodic EPD using  $\text{Mg}(\text{NO}_3)_2$  for various durations. Movies for the demonstration of robustness test using stainless-steel forks and a plastic eraser. These materials are available free of charge via the Internet at <http://pubs.acs.org>.

## ■ AUTHOR INFORMATION

### Corresponding Author

\*E-mail: kktgr@hiroshima-u.ac.jp.

### ORCID

Kiyofumi Katagiri: 0000-0002-9548-9835

Naoki Tarutani: 0000-0003-0696-8082

Kei Inumaru: 0000-0001-6876-3854

Tetsuo Uchikoshi: 0000-0003-3847-4781

Takahiro Seki: 0000-0003-3010-2641

Yukikazu Takeoka: 0000-0002-1406-0704

### Notes

The authors declare no competing financial interest.

### Author Contributions

The manuscript was written through contributions of all authors. All authors have given approval to the final version of the manuscript.

## ■ ACKNOWLEDGMENT

This work was supported by JSPS KAKENHI Grant Number JP18K19132, JP19H04699, JP20H02439. We thank Edanz Group (<https://en-author-services.edanzgroup.com/>) for editing a draft of this manuscript.

## ■ REFERENCES AND NOTES

- (1) Faulkner, E. B.; Schwartz, R. J. *High Performance Pigments 2nd ed.*; Wiley-VCH: Weinheim, 2009.
- (2) Luo, M. R., Ed. *Encyclopedia of Color Science and Technology*; Springer, New York, NY, 2016.
- (3) Buxbaum, G.; Pfaff, G. *Industrial Inorganic Pigments. 3rd ed.*; Wiley-VCH: Weinheim, 2005.
- (4) Gilani, S.H.; Marano, M. Chromium Poisoning and Chick Embryogenesis. *Environ. Res.* **1979**, *19*, 427–431.
- (5) Rustagi, N.; Singh, R. Mercury and Health Care. *Indian J. Occup. Environ. Med.* **2010**, *14*, 45–48.
- (6) Rice, K. M.; Walker, E. M., Jr.; Wu, M.; Gillette, C.; Blough, E. R. Environmental Mercury and Its Toxic Effects. *J. Prev. Med. Public Health* **2014**, *47*, 74–83.
- (7) Turner, A. Cadmium Pigments in Consumer Products and Their Health Risks. *Sci. Total Environ.* **2019**, *657*, 1409–1418.
- (8) Wani, A. L.; Ara, A.; Usmani, J. A. Lead Toxicity: A Review. *Interdiscip. Toxicol.* **2015**, *8*, 55–64.
- (9) E.U. Parliament, EU Council. Directive 2002/95/EC of the European Parliament and of the Council on the Restriction of the Use of Certain Hazardous Substances in Electrical and Electronic Equipment. *Off. J. Eur. Union.* **2003**, *46*, 19–23.
- (10) Jansen, M.; Letschert, H. P. Inorganic Yellow-Red Pigments without Toxic Metals. *Nature* **2000**, *404*, 980–982.

- (11) Tomczak, J. M.; Pourovskii, L. V.; Vaugier, L.; Georges, A.; Biermann, S. Rare-Earth Vs. Heavy Metal Pigments and Their Colors from First Principles. *Proc. Natl. Acad. Sci. USA*, **2013**, *110*, 904–907.
- (12) Kinoshita, S.; Yoshioka, S.; Miyazaki, J. Physics of Structural Colors. *Rep. Prog. Phys.* **2008**, *71*, 076401.
- (13) Takeoka, Y. Angle-Independent Structural Coloured Amorphous Arrays. *J. Mater. Chem.* **2012**, *22*, 23299–23309.
- (14) Zhao, Y. J.; Xie, Z. Y.; Gu, H.C.; Zhu, C.; Gu, Z. Z. Bio-Inspired Variable Structural Color Materials. *Chem. Soc. Rev.* **2012**, *41*, 3297–3317.
- (15) Dumanli, A. G.; Savin, T. Recent Advances in the Biomimicry of Structural Colours. *Chem. Soc. Rev.* **2016**, *45*, 6698–6724.
- (16) Fu, Y. L.; Tippetts, C. A.; Donev, E. U.; Lopez, R. Structural Colors: from Natural to Artificial Systems. *WIREs Nanomed. Nanobiotechnol.* **2016**, *8*, 758–775.
- (17) Kohri, M. Artificial Melanin Particles: New Building Blocks for Biomimetic Structural Coloration. *Polym. J.* **2019**, *51*, 1127–1135.
- (18) Fudouzi, H.; Xia, Y. Colloidal Crystals with Tunable Colors and Their Use as Photonic Papers. *Langmuir* **2003**, *19*, 9653–9660.
- (19) Shang, G.; Maiwald, L.; Renner, H.; Jalas, D.; Dosta, M.; Heinrich, S.; Petrov, A.; Eich, M. Photonic Glass for High Contrast Structural Color. *Sci. Rep.* **2018**, *8*, 7804.
- (20) Xiao, M.; Li, Y.; Allen, M. C.; Deheyn, D. D.; Yue, X.; Zhao, J.; Gianneschi, N. C.; Shawkey, M. D.; Dhinojwala, A. Bio-Inspired Structural Colors Produced via Self-Assembly of Synthetic Melanin Nanoparticles. *ACS Nano* **2015**, *9*, 5454–5460.

- (21) Wang, Z. Y.; Zhang, J. H.; Wang, Z. H.; Shen, H. Z.; Xie, J.; Li, Y. F.; Lin, L.; Yang, B. Biochemical-to-Optical Signal Transduction by pH Sensitive Organic–Inorganic Hybrid Bragg Stacks with a Full Color Display. *J. Mater. Chem. C* **2013**, *1*, 977–983.
- (22) Pi, J. K.; Yang, J.; Zhong, Q.; Wu, M. B.; Yang, H. C.; Schwartzkopf, M.; Roth, S. V.; Muller-Buschbaum, P.; Xu, Z. K. Dual-Layer Nanofilms via Mussel-Inspiration and Silication for Non-Iridescent Structural Color Spectrum in Flexible Displays. *ACS Appl. Nano Mater.* **2019**, *2*, 4556–4566.
- (23) Fan, W.; Zeng, J.; Gan, Q. Q.; Ji, D. X.; Song, H. M.; Liu, W. Z.; Shi, L.; Wu, L. M. Iridescence-Controlled and Flexibly Tunable Retroreflective Structural Color Film for Smart Displays. *Sci. Adv.* **2019**, *5*, eaaw8755.
- (24) Kim, J. H.; Moon, J. H.; Lee, S. Y.; Park, J. Biologically Inspired Humidity Sensor Based on Three-Dimensional Photonic Crystals. *Appl. Phys. Lett.* **2010**, *97*, 103701.
- (25) Qin, M.; Sun, M.; Hua, M. T.; He, X. M. Bioinspired Structural Color Sensors Based on Responsive Soft Materials. *Cur. Opin. Solid State Mater. Sci.* **2019**, *23*, 13–27.
- (26) Ge, D. T.; Lee, E.; Yang, L. L.; Cho, Y. G.; Li, M.; Gianola, D. S.; Yang, S. A Robust Smart Window: Reversibly Switching from High Transparency to Angle - Independent Structural Color Display. *Adv. Mater.* **2015**, *27*, 2489–2495.
- (27) Lee, K. T.; Han, S. Y.; Li, Z. J.; Baac, H. W.; Park, H. J. Flexible High-Color-Purity Structural Color Filters Based on a Higher-Order Optical Resonance Suppression. *Sci. Rep.* **2019**, *9*, 14917.
- (28) Nam, H.; Song, K.; Ha, D.; Kim, T. Inkjet Printing Based Mono-layered Photonic Crystal Patterning for Anti-counterfeiting Structural Colors. *Sci. Rep.* **2016**, *6*, 30885.

- (29) Ma, W.; Kou, Y. S.; Zhao, P.; Zhang, S. F. Bioinspired Structural Color Patterns Derived from 1D Photonic Crystals with High Saturation and Brightness for Double Anti-Counterfeiting Decoration. *ACS Appl. Polym. Mater.* **2020**, *2*, 1605–1613.
- (30) Stöber, W.; Fink, A.; Bohn, E. Controlled Growth of Monodisperse Silica Spheres in the Micron Size Range. *J. Colloid Interface Sci.* **1968**, *26*, 62–69.
- (31) Liu, P. M.; Bai, L.; Yang, J. J.; Gu, H. C.; Zhong, Q. F.; Xie, Z. Y.; Gu, Z. Z. Self-Assembled Colloidal Arrays for Structural Color. *Nanoscale Adv.* **2019**, *1*, 1672–1685.
- (32) Liu, T. Y.; VanSaders, B.; Glotzer, S. C.; Solomon, M. J. Effect of Defective Microstructure and Film Thickness on the Reflective Structural Color of Self-Assembled Colloidal Crystals. *ACS Appl. Mater. Interfaces* **2020**, *12*, 9842–9850.
- (33) Yi, B.; Shen, H. F. Facile Fabrication of Crack-Free Photonic Crystals with Enhanced Color Contrast and Low Angle Dependence. *J. Mater. Chem. C* **2017**, *5*, 8194–8200.
- (34) Ge, D. T.; Yang, X. M.; Chen, Z.; Yang, L. L.; Wu, G. X.; Xia, Y.; Yang, S. Colloidal Inks from Bumpy Colloidal Nanoparticles for the Assembly of Ultrasmooth and Uniform Structural Colors. *Nanoscale* **2017**, *9*, 17357–17363.
- (35) Torres, L.; Margaronis, A.; Meinhardt, B. M. B.; Granzow, L.; Ayyub, O. B.; Kofinas, P. Rapid and Tunable Method To Fabricate Angle-Independent and Transferable Structurally Colored Films. *Langmuir* **2020**, *36*, 1252–1257.
- (36) Takeoka, Y.; Yoshioka, S.; Takano, A.; Arai, S.; Nueangnoraj, K.; Nishihara, H.; Teshima, M.; Ohtsuka, Y.; Seki, T. Production of Colored Pigments with Amorphous Arrays of Black and White Colloidal Particles. *Angew. Chem. Int. Ed.* **2013**, *52*, 7261–7265.

- (37) Kohri, M.; Nannichi, Y.; Taniguchi, T.; Kishikawa, K. Biomimetic Non-Iridescent Structural Color Materials from Polydopamine Black Particles that Mimic Melanin Granules. *J. Mater. Chem. C* **2015**, *3*, 720–724.
- (38) Van der Biest, O. O.; Vandeperre, L. J.: Electrophoretic Deposition of Materials. *Annu. Rev. Mater. Sci.* **1999**, *29*, 327–352.
- (39) Corni, I.; Ryan, M. P.; Boccaccini, A. R. Electrophoretic Deposition: From Traditional Ceramics to Nanotechnology. *J. Eur. Ceram. Soc.* **2008**, *28*, 1353–1367.
- (40) Dickerson, J. H.; Boccaccini A. R., Eds. *Electrophoretic Deposition of Nanomaterials* Springer, New York, NY, 2012.
- (41) Nguyen, N. T. K.; Renaud, A.; Dierre, B.; Bouteille, B.; Wilmet, M.; Dubernet, M.; Ohashi, N.; Grasset, F., Uchikoshi, T. Extended Study on Electrophoretic Deposition Process of Inorganic Octahedral Metal Clusters: Advanced Multifunctional Transparent Nanocomposite Thin Films. *Bull. Chem. Soc. Jpn.* **2018**, *91*, 1763–1774.
- (42) Saito, N.; Yanada, K.; Kondo, Y. Azobenzene-Based Iustrous Golden Thin Films Fabricated by Electrophoreticdeposition. *Colloid Surf. A* **2019**, *579*, 123705.
- (43) Katagiri, K.; Tanaka, Y.; Uemura, K.; Inumaru, K.; Seki, T.; Takeoka, Y. Structural Color Coating Films Composed of an Amorphous Array of Colloidal Particles via Electrophoretic Deposition. *NPG Asia Mater.* **2017**, *9*, e355.
- (44) Katagiri, K.; Uemura, K.; Uesugi, R.; Inumaru, K.; Seki, T.; Takeoka, Y. Structurally Colored Coating Films with Tunable Iridescence Fabricated via Cathodic Electrophoretic Deposition of Silica Particles. *RSC Adv.* **2018**, *8*, 10776–10784.
- (45) Li, Q. S.; Zhang, Y. F.; Shi, L.; Qiu, H. H.; Zhang, S. M.; Qi, N.; Hu, J. C.; Yuan, W.; Zhang, X. H.; Zhang, K. Q. Additive Mixing and Conformal Coating of Noniridescent

- Structural Colors with Robust Mechanical Properties Fabricated by Atomization Deposition. *ACS Nano* **2018**, *12*, 3095–3102.
- (46) Meng, F.; Umair, M. M.; Iqbal, K.; Jin, X.; Zhang, S.; Tang, B. Rapid Fabrication of Noniridescent Structural Color Coatings with High Color Visibility, Good Structural Stability, and Self-Healing Properties. *ACS Appl. Mater. Interfaces* **2019**, *11*, 13022–13028.
- (47) Meng, Y.; Tang, B. T.; Xiu, J. H.; Zheng, X. X.; Ma, W.; Ju, B. Z.; Zhang, S. F. Simple Fabrication of Colloidal Crystal Structural Color Films with Good Mechanical Stability and High Hydrophobicity. *Dyes Pigm.* **2015**, *123*, 420–426.
- (48) Meng, Y.; Tang, B. T.; Ju, B. Z.; Wu, S. L.; Zhang, S. F. Multiple Colors Output on Voile through 3D Colloidal Crystals with Robust Mechanical Properties. *ACS Appl. Mater. Interfaces* **2017**, *9*, 3024–3029.
- (49) Shen, H. F.; Liang, Q. M.; Song, L. J.; Chen, G. W.; Pei, Y. B.; Wu, L. B.; Zhang, X. Y. Facile Fabrication of Mechanically Stable Non-Iridescent Structural Color Coatings. *J. Mater. Sci.* **2020**, *55*, 2353–2364.
- (50) Echeverri, M.; Patil, A.; Xiao, M.; Li, W. Y.; Shawkey, M. D.; Dhinojwala, A. Developing Noniridescent Structural Color on Flexible Substrates with High Bending Resistance. *ACS Appl. Mater. Interfaces* **2019**, *11*, 21159–21165.
- (51) Pashley, R. M.; Israelachvili, J. N. DLVO and Hydration Forces between Mica Surfaces in  $Mg^{2+}$ ,  $Ca^{2+}$ ,  $Sr^{2+}$ , and  $Ba^{2+}$  Chloride Solutions. *J. Colloid Interface Sci.* **1984**, *97*, 446–455.

- (52) Ruiz-Cabello, F. J. M.; Trefalt, G.; Csendes, Z.; Sinha, P.; Oncsik, T.; Szilagyi, I.; Maroni, P.; Borkovec, M. Predicting Aggregation Rates of Colloidal Particles from Direct Force Measurements. *J. Phys. Chem. B* **2013**, *117*, 11853–11862.
- (53) Zohar, O.; Leizeron, I.; Sivan, U. Short Range Attraction between Two Similarly Charged Silica Surfaces. *Phys. Rev. Lett.* **2006**, *96*, 177802.
- (54) Russ, B. E.; Talbot, J. B. An Analysis of the Binder Formation in Electrophoretic Deposition. *J. Electrochem. Soc.* **1998**, *145*, 1253–1256.
- (55) Ropp, R. C. *Encyclopedia of the Alkaline Earth Compounds*; Elsevier: Oxford, 2013.
- (56) Izaki, M.; Omi, T. Electrolyte Optimization for Cathodic Growth of Zinc Oxide Films. *J. Electrochem. Soc.* **1996**, *143*, L53–L55.
- (57) Shinagawa, T.; Watase, S.; Izaki, M. Size-Controllable Growth of Vertical ZnO Nanorod Arrays by a Pd-Catalyzed Chemical Solution Process. *Cryst. Growth Des.* **2011**, *11*, 5533–5539.

## Table of Contents (TOC) Graphic

